

See discussions, stats, and author profiles for this publication at: <https://www.researchgate.net/publication/227935584>

Intracranial oscillations of cerebrospinal fluid and blood flows: Analysis with magnetic resonance imaging

ARTICLE *in* JOURNAL OF MAGNETIC RESONANCE IMAGING · MARCH 2002

Impact Factor: 3.21 · DOI: 10.1002/jmri.10084

CITATIONS

28

READS

97

5 AUTHORS, INCLUDING:



Uwe Klose

University of Tuebingen

265 PUBLICATIONS 5,218 CITATIONS

SEE PROFILE



Herwig Strik

Philipps University of Marburg

76 PUBLICATIONS 904 CITATIONS

SEE PROFILE



Wolfgang Grodd

RWTH Aachen University

21 PUBLICATIONS 178 CITATIONS

SEE PROFILE

Intracranial Oscillations of Cerebrospinal Fluid and Blood Flows: Analysis With Magnetic Resonance Imaging

Claudia Strik, MD,^{1*} Uwe Klose, PhD,¹ Michael Erb, PhD,¹ Herwig Strik, MD,² and Wolfgang Grodd, MD¹

Purpose: To detect oscillations of the cerebrospinal fluid (CSF) flow related to the heartbeat and frequencies lower than 0.6 Hz and to compare these oscillations of CSF and blood flow in cerebral vessels by using echo planar imaging in real time mode. The existence of such waves has been well known but has not yet been shown by MRI.

Materials and Methods: In a slice perpendicular to the aqueduct, CSF flow as well as CBF, could be determined in sagittal sinus, basilar artery, and capillary vessels. After Fourier analysis, four frequency bands were assigned.

Results: In the very high-frequency (heart rate) range, the integrals under the CSF curves were more closely related to arterial CBF than to changes in the sinus. Also, in the high-frequency (respiration rate), low-frequency (0.05–0.15 Hz), and very-low-frequency (0.008–0.05 Hz) ranges, the integrals under the CSF curves corresponded with arterial and capillary CBF.

Conclusion: Slow and fast oscillations in CSF flow are detectable in healthy persons with a proportional allotment to arterial and capillary CBF.

Key words: cerebrospinal fluid; cerebral blood flow; magnetic resonance imaging; spectrum analysis; rhythmic oscillations

J. Magn. Reson. Imaging 2002;15:251–258.
© 2002 Wiley-Liss, Inc.

RHYTHMIC OSCILLATIONS WITH LOW frequencies below the heart rate were first described during arterial blood pressure monitoring by Hering, Traube, and Mayer as early as the 19th century (1–3). Subsequently, similar fluctuations were observed in various other physiological and pathological parameters, such as

heart rate variability, cerebral blood flow (CBF) velocity, and vessel diameter variation (4–6).

In the cranium, slow oscillations of varying frequencies were first documented in association with intracranial pressure (ICP) measurements. The distinction between B-waves with a frequency of 0.5–2/minute and C-waves with a range of 4–8/minute was first introduced by Lundberg (7). Subsequently, corresponding cerebral oscillations were found in studies of blood flow (8) and blood flow velocity (9). Prior to magnetic resonance imaging (MRI), intracranial slow rhythmic oscillations were detectable only by invasive intracranial pressure measurement or, in the case of CBF, by non-invasive Doppler measurements.

Pulsation and flow of the cerebrospinal fluid (CSF) are closely linked to the changes in the CBF induced by the heartbeat and by respiration. These have been described in a number of MRI studies, but additional slow oscillations within the CSF—detectable with MRI—have not been reported. The majority of the studies of CSF flow are based on cardiac-gated MRI and have used gradient echo sequences and averaging of repetitive CSF signals to identify distinct frequencies and waveforms. With this averaging technique, a pulsatile character of CSF flow within the aqueduct was repeatedly demonstrated with a systolic down and diastolic up movement of the CSF (10,11). However, ECG-gated examinations are largely restricted to CSF oscillations in the range of the heart rate.

Additional influences of the respiration can be observed if an echo-planar imaging (EPI) sequence is used (12). To detect slower rhythmic oscillations within the CSF motion, real-time techniques are necessary and any kind of averaging has to be avoided. The EPI technique allows such real-time recording with a high temporal and satisfactory spatial resolution over a longer time period (minutes). With this technique, slow physiologic signal variations have already been found in the brain parenchyma, but they were usually considered as a physiological noise (13). In the study described here, we show that EPI is suitable for the analysis of slow signal variations in CSF, cerebral vessels, and brain parenchyma.

¹Section of Experimental MR of the CNS, Department of Neuroradiology, University of Tuebingen, Germany.

²Department of Neurology, University of Goettingen, Germany.

Contract grant sponsor: Deutsche Forschungsgemeinschaft; Contract grant number: Kl 1093/3-1.

A part of our study was presented at the 11th International Symposium on Intracranial Pressure in Cambridge, UK, in July 2000.

*Address reprint requests to: C.S., Auf dem Lohberge 14, D-37085 Goettingen, Germany. E-mail: CStrik@AOL.com

Received February 20, 2001; Accepted November 30, 2001.

MATERIALS AND METHODS

Thirteen healthy volunteers were examined after having given their informed written consent, knowing about all the examination procedures. Two of them were excluded from further statistical evaluation because of movement artifacts. The remaining five females and six males (mean age, 28 years; range, 7–37 years) had no severe diseases in their medical histories and no recent chronic diseases, such as arterial hypertension or lung disease, according to an informal interview. Except for two minor contusions to the skull, no traumatic brain injury was reported. Nine volunteers were examined in the evening (6–11 P.M.), the two others in the afternoon (4–6 P.M.).

Measurements were performed with dynamic EPI technique with a conventional 1.5-T MR system (Siemens Vision, Erlangen, Germany) (14). The head was positioned in a circular polarized head coil. To enable an exact acquisition of data from the oscillating CSF, an axial slice was tilted and adjusted to a perpendicular orientation toward the aqueduct of Sylvii, which was identified in the midsagittal plane of a scout image (Fig. 1a). This semicoronal slice also enabled the identification of the superior sagittal sinus and basilar artery, as well as regions of the brain parenchyma. The data were recorded with a field of view (FOV) of 120×120 mm, a slice thickness of 3 mm, and a TE of 43 msec. The flip angle was 90° , and the matrix was 64×64 . The time resolution of successive images was 156 msec. In each examination, 3072 acquisitions were performed, with a total time period of 8 minutes.

Simultaneously with the registration of MRI signals, the peripheral pulse was monitored with a pulse oximeter (Nonin 8600 FO, Nonin Medical Inc., Plymouth, MN) mounted on the right index finger and the respiration rate was measured with a respiration belt. These physiological data were recorded and stored with a separate computer, together with a trigger signal from the MR system, to enable the retrospective synchronization of data during postprocessing.

Using the peripherally measured pulse instead of the electrocardiogram (ECG) signal might result in slightly different delays between the individuals. This delay, however, has no effect on the intended frequency analysis of signal variations within CSF spaces and vessels.

Systemic arterial blood pressure was monitored intermittently every 2 minutes on the left upper arm with an automatic oscillatory device (Dinamap 1246, Critikon, Norderstedt, Germany), in seven volunteers simultaneously and in three volunteers before and after the measurement in a sitting position.

Postprocessing of the data was performed at a separate workstation (Indigo, Silicon Graphics, Mountain View, CA) with an in-house-developed software application (BiKe) and with self-designed evaluation procedures using PVWAVE (Visual Numeric, Boulder, CO). The program BiKe allows the visualization of images series, the calculation of various parameter maps, and the separation of signal intensities within selected regions of interest (ROIs) or pixels into one-dimensional data arrays. Further analysis of data was performed with Pulsatio. This program allows the reading of data

arrays with signal intensities provided by BiKe, together with the files containing the information about respiration and cardiac pulses. These physiological data were transformed using the MR trigger data to provide a single value for each acquired image. The time delay to the last obtained cardiac pulse was used to characterize the heart function. All these data were Fourier transformed after subtraction of the mean value and Hanning filtering. The area below the resulting curve was evaluated in predefined frequency ranges.

Using BiKe, all 3072 images were viewed in a cine mode for a first visual control of CSF pulsations and to depict movement artifacts. Due to this control, two of the volunteer studies had to be excluded due to considerable head motions. Next, the SD in each pixel was used to calculate a signal variation map of the examined slice. In this map then, the following ROIs ($3\text{--}30$ pixels) were selected: 1) aqueduct of Sylvii, 2) superior sagittal sinus, 3) basilar artery anterior to the brain stem, and two parenchymal brain regions: one in the 4) brain stem, the other in the 5) parietal lobe (Fig. 1b). The signal variations of these ROI were taken as raw data for further analysis, as displayed (Fig. 1c). All data from brain tissue, CSF, and arterial and venous MRI signals were evaluated, together with the physiological recordings from the pulse oximeter and respiration belt in the time domain for a first descriptive analysis.

For a spectral evaluation with frequency analysis, the integrals of four different frequency ranges—as mentioned below—were calculated for the different ROI (aqueduct, artery, vein, and brain parenchyma), as well as for the heart rate variability.

As no general consensus on the classification of slow oscillations exists, we have introduced an arbitrary classification similar to the one used in a previous study with the Doppler technique (15) by dividing the whole registered spectrum ($0.001\text{--}6.4$ Hz) into two distinct frequency ranges: a slow frequency range and a higher (heart action-related) frequency range. The frequency range of heart rate, classified as very high frequency, was restricted to the first harmonic and had a bandwidth of 1.1 Hz. The slow frequency range below the heart rate was then subdivided in three domains: high frequency (>0.15 Hz), low frequency ($0.05\text{--}0.15$ Hz), and very low frequency ($0.008\text{--}0.05$ Hz). As respiration rate varied from subject to subject, we recorded the respiration excursion with a respiration belt and could thus determine the exact frequency for each individual subject. The bandwidth also varied from subject to subject; thus we chose a fixed bandwidth of 0.42 Hz symmetric to the individual main frequency peak to allow for a group data comparison.

To estimate the correlation of physiological parameters with the ROI signal intensity course, i.e., the influence of heart rate on CSF oscillations, the percentage of very-high-frequency signals related to the signal of all four frequency ranges in the CSF was determined by calculating the integral of each band of frequencies. As a control for this evaluation procedure, we compared the percentage of the different frequency bands of the heart rate with the signal variation in the basilar artery.

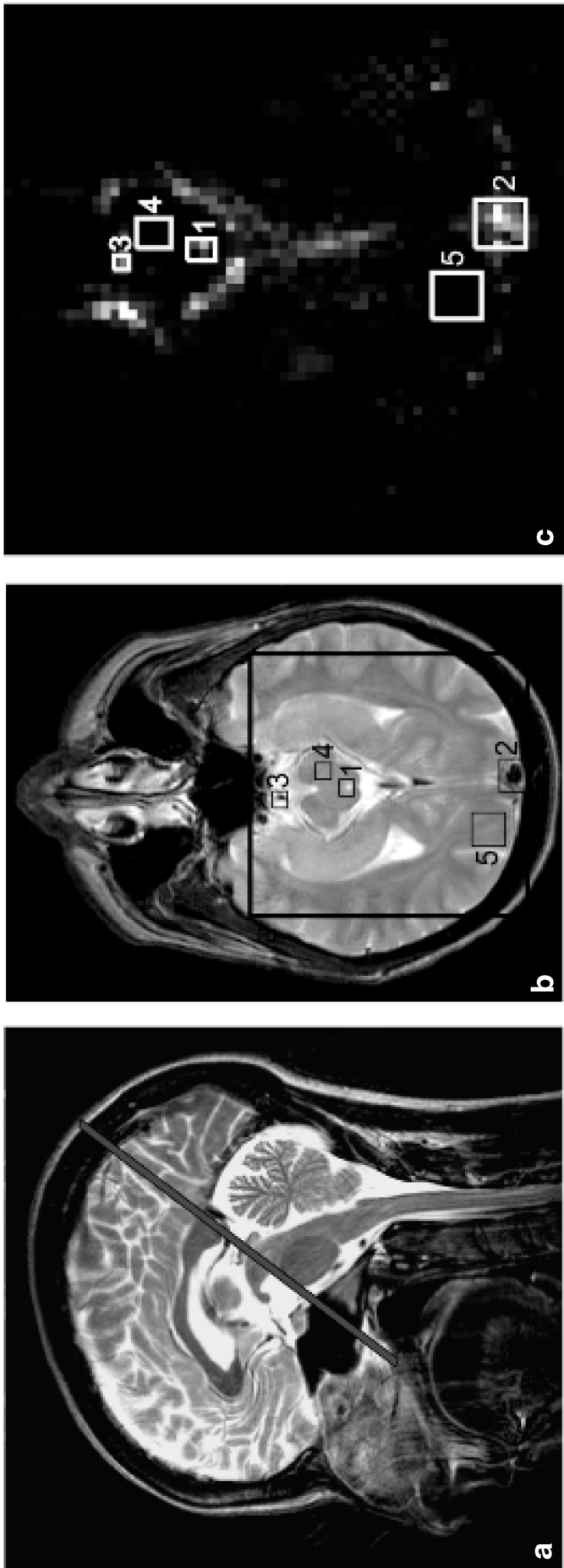


Figure 1. a: Midsagittal slice with the position of the slice of the dynamic measurement marked. **b:** T2-weighted image with slice orientation as in dynamic measurement: region of aqueduct of Sylvii (1), region of superior sagittal sinus (2), region of basilar artery (3), parenchyma of brain stem (4), and parietal lobe (5). **c:** Parameter map with the ROIs: region of aqueduct of Sylvii (1), region of superior sagittal sinus (2), region of basilar artery (3), parenchyma of brain stem (4), and parietal lobe (5).

This comparison served as a plausibility standard for which a close correlation was assumed.

For comparison of the spectra with data from previous MRI studies, the proportion of very high, heart rate-related frequencies was calculated as a percentage of the whole spectrum recorded. The various slow frequencies were then analyzed separately for their percentage of the spectrum of slow waves only, corresponding to previous studies with the Doppler technique (16).

RESULTS

In Figure 1a, the midsagittal scout image with the marked slice for the EPI measurement and a semicoronal T2-weighted image are displayed to depict details of the accessible anatomy (Fig. 1b).

The aqueduct (3–9 pixels) and the superior sagittal sinus (4–20 pixels) could be distinguished in all volunteers. In 10 persons, the basilar artery (single pixel) in the vicinity of the aqueduct could be identified with confidence. In one volunteer, the carotid artery was chosen instead of the basilar artery because no adequate signal of the latter could be achieved. In all volunteers, two regions of brain tissue were selected (25–30 pixels), one in the left part of the brain stem and one in the right parietal region. In one volunteer, the data of the pulse oximeter were not usable because of cable dislocation.

With time-domain analysis, signal variations from the CSF, brain parenchyma, and cerebral arterial and venous blood vessels observed in each volunteer were compared with heart rate (interpulse interval) and respiration. A representative result for the signal variations in the CSF, the superior sagittal sinus, the basilar artery, and the brain parenchyma, together with the interpulse interval and respiration rate from a 26-year-old volunteer, is given in Figure 2. While slow rhythmic variations are masked in the CSF and the basilar artery due to large signal fluctuations, additional signal variations of frequencies below the respiration are clearly visible in the sagittal sinus and—less pronounced—in the brain stem.

The corresponding spectral analysis is given in Figure 3. Here all ROIs—with the exceptions of respiration and brain parenchyma—showed a distinct dominance of the very high frequency. The sidebands of the very high frequency originate from the respiration and are more prominent in the CSF and artery than in the sagittal sinus and brain tissue. In the CSF and in the artery, the high frequency is clearly visible. In the sagittal sinus as well as in the brain parenchyma, the high frequency is difficult to recognize. The low and very low frequencies in the sagittal sinus and the very low frequency in the brain stem are much more pronounced than those in the heart rate variability and signal variation of the artery and CSF.

The integral of the very-high-frequency range within the spectrum was evaluated in relation to all four spectra (very high, high, low, and very low frequencies). In Figure 4, the total range, the 25th and 75th percentiles, and the median of the very high frequency in all parameters are demonstrated. In all evaluated regions, the

average contribution of the very-high-frequency range was more than 50%. The pulse wave was less (58.2%) pronounced in the sagittal sinus than in the brain parenchyma (71.8%), CSF (81.9%), and artery (83.8%). The evaluation of the other frequency ranges was performed in relation to the integral of all evaluated spectra, excluding the very-high-frequency range. As shown in Figure 5a, the high frequencies—corresponding to respiration—had a proportion of 55.0% of the slow oscillations in the CSF. Similarly, these high frequencies accounted for 54.2% of the arterial signal, 53.3% of the heart rate variability, and 50.8% of the brain parenchyma signal, but for only 22.0% of the venous signal.

Low frequencies—corresponding to Mayer waves—(Fig. 5b) were detected with a proportion of 26.9% of CSF oscillations, 30.0% of the arterial signal, 30.6% of the heart rate variability, and 30.2% of brain parenchyma oscillations, but of 42.6% of the frequencies in the venous sinus.

Very low frequencies—corresponding to B-waves—accounted for 18.2% of the CSF flow, 17.2% of the arterial signal, 15.8% of the heart rate variability, and 18.7% of brain parenchyma oscillations, but for 35.5% of the venous signal (Fig. 5c).

DISCUSSION

Although there is no separate pumping mechanism for the CSF, the pulsatile character of its flow is well known. This may not only be caused by the vicinity of CSF-containing space to blood vessels. In the fixed intracranial space, the volume of a low-pressure system like the CSF is thought to be reduced when higher pressure fluid enlarges its intracranial volume, like arterial blood during systole (Monro-Kelly Doctrine). Factors influencing arterial and venous blood flow, such as heart rate, blood pressure, and respiration, are also of considerable importance for CSF flow (17).

While CBF can be examined efficiently with the transcranial Doppler technique, noninvasive recording of CSF flow in adults is restricted to the MRI technique. However, analysis of the whole spectrum of physiological CSF oscillations requires a real-time method with a long measurement period and a high time resolution above 1 Hz to enable detection of all oscillations and to avoid aliasing of cardiac-related signal changes. The method described here, based on the EPI technique, allows 8 minutes of real-time recording of CSF movement in a noninvasive manner, with a time resolution of 156 msec and simultaneous registration of the heart rate and respiration. The obtained images show a strong signal enhancement of nuclei flowing into the slice between successive measurements, as a flip angle of 90° was used. Other than with unidirectional flow, a signal reduction will occur with oscillating movements like in the CSF within the aqueduct or periodically moving brain tissue, due to a complex spin saturation history. This effect reduces the obtained signal intensity and prevents a quantitative analysis of flow velocities. Nevertheless, the examination of frequency components of signal variations should be less affected by these saturation effects.

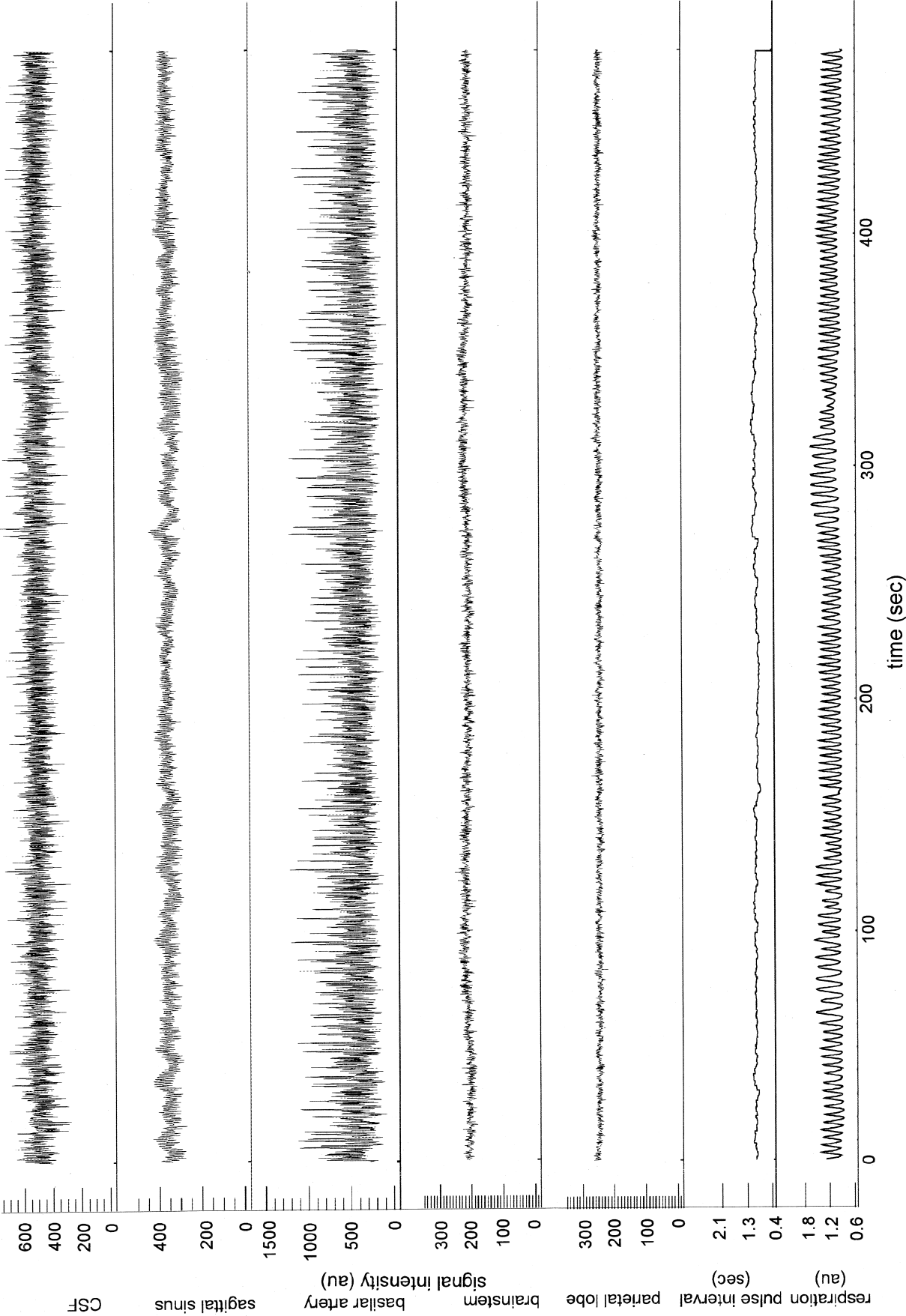


Figure 2. A 26-year-old volunteer. Time domain analysis with signal variation curve in CSF, venous blood, arterial blood, capillary blood flow in brain stem and parietal lobe, peripheral pulse interval, and respiration curve.

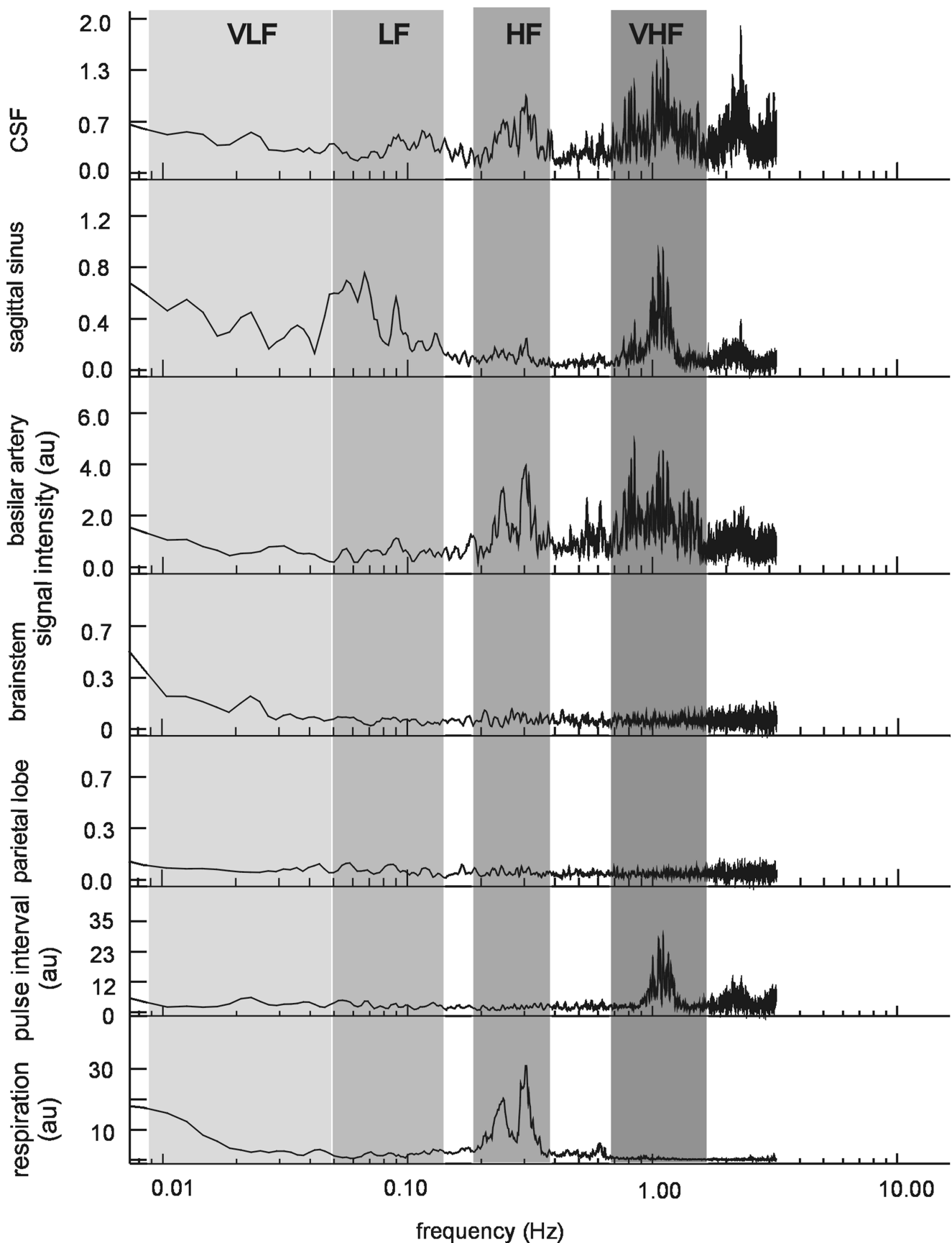


Figure 3. A 26-year-old volunteer. Corresponding spectral analysis of signal intensity in CSF flow, venous blood flow, arterial blood flow, capillary blood flow in brain stem and parietal lobe, peripheral pulse interval, and respiration curve. The different frequency bands are marked with a colored background. sec, seconds; a.u., arbitrary units; VLF, very low frequency; LF, low frequency; HF, high frequency; VHF, very high frequency.

In the study presented here, we focused on low and very low CSF oscillations and analyzed their correlation with cerebral arterial and venous blood flow, heart rate, and respiration.

The spectral analysis of the four analyzed frequencies of oscillations revealed similar proportions of arterial signal, heart rate, and CSF oscillations, supporting the assumption that CSF flow is primarily determined by heart action. Corresponding proportions of frequencies were observed with all slow oscillations of the brain parenchyma, while the proportions of very high, heart-related frequencies were slightly different from the other parameters. It can be presumed that changes of arterial blood volume have a major influence on CSF flow, as well as on oscillations of the brain parenchyma. Marked differences to the other results were observed with the venous signal, which contained a considerably smaller proportion of heart rate- and respiration-related oscillations, but a considerably higher proportion of low and very low frequencies, compared with all the other parameters (Fig. 3). The fixed diameter of the incompressible venous sinus may be one reason for this minor influence of heart action; also, the capillary system and venules cause a deceleration of the pulse wave before it reaches the large cerebral veins. Respiratory effects on venous outflow via central venous pressure also seem to be of minor effect on oscillations in the venous sinus. The higher proportion of low and very low frequencies may reflect a venous autoregulatory mechanism, as proposed previously (18). Apart from the description of low pulsatility, no comparable data for the venous CBF exist in the literature.

Although corresponding fluctuations of CBF velocity were detected with transcranial Doppler (16), respiration-related frequencies were found to have only a minor influence (16%), as opposed to low-frequency (43%) and very-low-frequency (45%) components. There is no obvious reason for the discrepancy in our results. Our results of the arterial blood flow with the MR technique

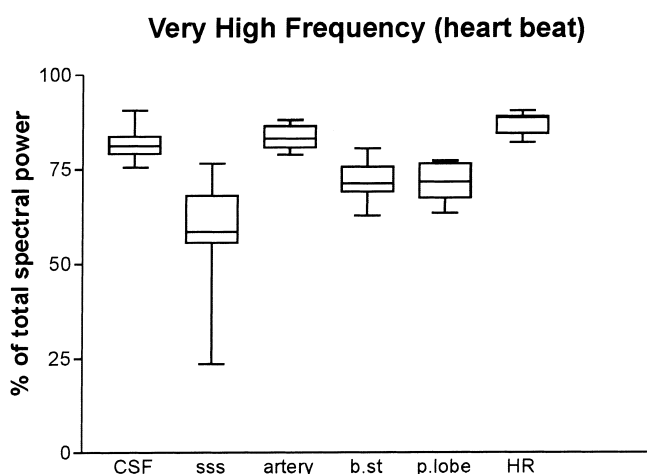


Figure 4. Range, 25th and 75th percentiles, and median of very high frequencies in artery, vein, heart rate variability, CSF, and parietal and brain stem parenchyma. sss, superior sagittal sinus; b.st., brain stem parenchyma; p.lobe, parietal lobe; HR, heart rate.

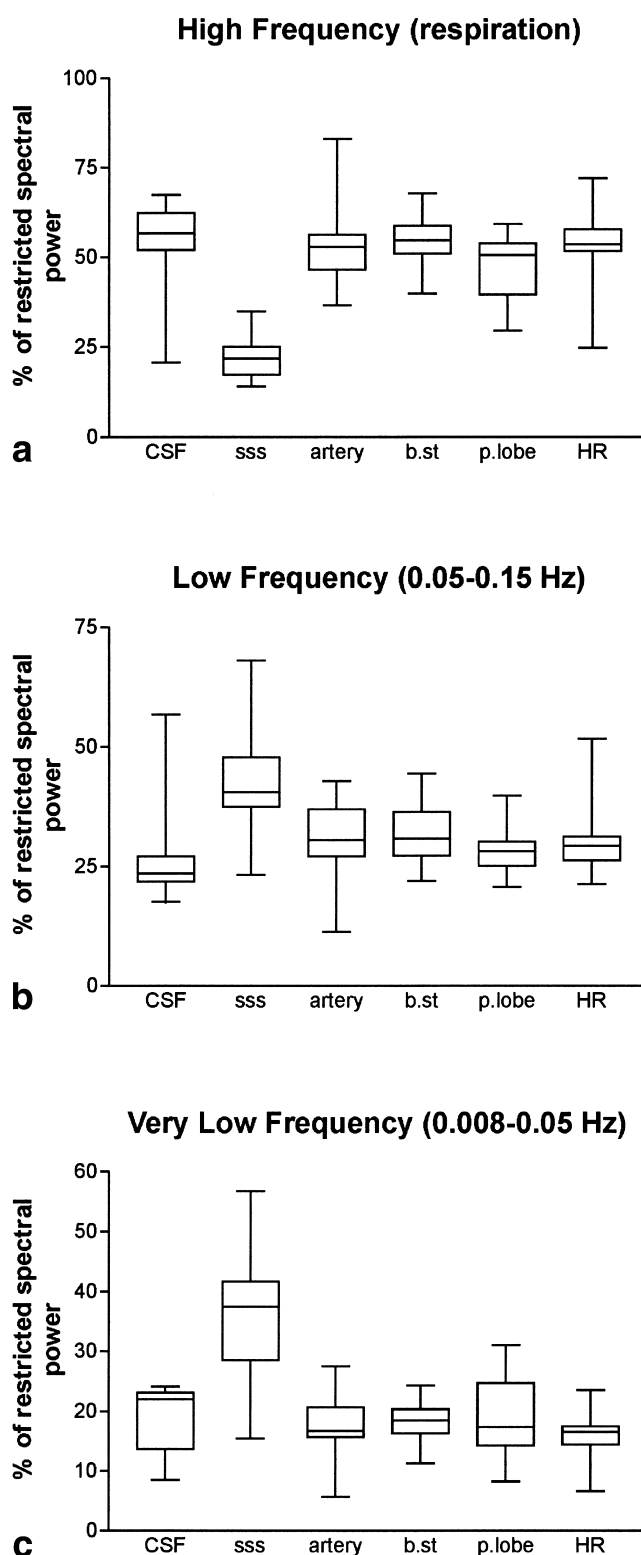


Figure 5. Range, 25th and 75th percentiles, and median of high (a), low (b), and very low (c) frequencies in artery, vein, heart rate variability, CSF, and parietal and brain stem parenchyma. sss, superior sagittal sinus; b.st., brain stem parenchyma; p.lobe, parietal lobe; HR, heart rate.

are comparable with the results of the heart rate variability with the pulse oximeter. The results of transcranial doppler (TCD) measurement are comparable with the arterial blood pressure (ABP) results. Different ex-

ternal conditions like supine position, circadian differences, considerable MR scanner noise, and data post-processing may account for different results in our study.

Intracranial pressure oscillations with a wavelength of 30–120 sec (= 0.008–0.04 Hz) were called B-waves by Lundberg and, similar to C-waves, considered as a pathological phenomenon. However, corresponding oscillations of CBF velocity were detected with TCD in healthy volunteers and called B-wave equivalents (9). The author's suggestion that these oscillations are physiological is supported by our detection of very low frequencies with each examined parameter of each volunteer.

Oscillations of the intracranial pressure with a frequency of 4–8/minute were originally called C-waves by Lundberg in 1960. Because C-waves have first been observed with raised intracranial pressure, they have been regarded as a pure pathologic phenomenon. Although C-waves in the CSF pressure have early been related to Mayer waves in the blood circulation and although the close correlation between blood and CSF oscillations is known, it is not yet sufficiently clarified whether C-waves occur also as a physiologic phenomenon, as supposed by Guillaume and Janny (1951), cited by Kjällquist et al (19). Our finding that slow signal intensity oscillations were observed in all volunteers supports the assumption that oscillations in the spectrum of C-waves or Mayer waves are entirely physiologic.

Oscillations of various frequencies of CSF flow and intracranial pressure and of CBF and brain parenchyma have been demonstrated in numerous studies with invasive and noninvasive methods. However, simultaneous recording of all parameters, with the major influence on CSF flow, and analysis of their intercorrelations could not be provided until recently. The method described here, based on EPI-MRI technique, allows for a noninvasive analysis of a wide range of CSF oscillations and their relation with the heart rate, cerebral arterial and venous blood flow, respiration, and oscillations of the brain parenchyma. Our observations in healthy individuals support the theory that these waves are physiological phenomena. In case an autonomous pacemaker for B-waves and Mayer waves exists, as assumed by several authors, with a location in the rostral medulla oblongata (5,15), modulations of these waveforms in pathologic conditions, such as raised pressure in the infratentorial space, could be expected. Further studies will have to clarify whether or not damage to the medulla oblongata results in changes of slow rhythmic oscillations.

ACKNOWLEDGMENTS

We are indebted to Dr. Appletree Rodden for his kind help with the English language.

REFERENCES

1. Mayer S. Studies about the physiology of heart and blood vessels [Studien zur Physiologie des Herzens und der Blutgefäße]. Sitzungsbericht der mathematisch-naturwissenschaftlichen Classe Wien 1876;74:281–307.
2. Traube L. About periodic actions of the vasomotor and inhibitory nerve center [Ueber periodische Thätigkeits-Aeusserungen des vasomotorischen und Hemmungs-Nervencentrums]. Centralblatt medizinischer Wissenschaften Berlin 1865;3:881–885.
3. Hering E. About the influence of respiration to the circulation. I. About respiratoric movements of the vessels system [Über den Einfluss der Athmung auf den Kreislauf I. Über Athembewegungen des Gefässsystems]. Sitzungsbericht der mathematisch-naturwissenschaftlichen Classe Wien 1869;60:829–856.
4. Auer LM, Sayama I. Intracranial pressure oscillations (B-waves) caused by oscillations in cerebrovascular volume. Acta Neurochir Wien 1983;68:93–100.
5. Einhäupl KM, Garner C, Dirnagl U, et al. Oscillations of ICP related to cardiovascular parameters. In: Miller JD, Teasdale GM, Rowan JO, Galbraith SL, Mendelow AD, editors. Intracranial pressure VI. Berlin Heidelberg: Springer-Verlag; 1986. p 290–297.
6. Elghozi JL, Japundzic N, Grichois ML, et al. Nervous mechanisms of spontaneous oscillations of systolic blood pressure and heart rate. Arch Mal Coeur Vaiss 1990;83:1065–1068.
7. Lundberg N. Continuous recording and control of ventricular fluid pressure in neurosurgical practice. Acta Psych Neurol Scand (Suppl) 1960;149:1–193.
8. Fasano VA. Intraoperative use of laser Doppler in the study of cerebral microvascular circulation. Acta Neurochir Wien 1988;95:40–48.
9. Mautner-Huppert D, Haberl RL, Dirnagl U, et al. B-waves in healthy persons. Neurol Res 1989;11:194–196.
10. Bergstrand G, Bergstrom M, Nordell B, et al. Cardiac gated MR imaging of cerebrospinal fluid flow. J Comput Assist Tomogr 1985; 9:1003–1006.
11. Mark AS, Feinberg DA, Sze GK, et al. Gated magnetic resonance imaging of the intracranial cerebrospinal fluid spaces. Acta Radiol Suppl Stockh 1986;369:296–299.
12. Klose U, Strik C, Kiefer C, et al. Detection of a relation between respiration and CSF pulsation with echoplanar technique. J Magn Reson Imaging 2000;11:438–444.
13. Biswal B, DeYoe AE, Hyde JS. Reduction of physiological fluctuations in fMRI using digital filters. Magn Reson Med 1996;35:107–113.
14. Klose U, Erb M, Wildgruber D, et al. Improvement of the acquisition of a large amount of MR images on a conventional whole body system. Magn Reson Imaging 1999;17:471–474.
15. Lang EW, Diehl RR, Timmermann L, et al. Spontaneous oscillations of arterial blood pressure, cerebral and peripheral blood flow in healthy and comatose subjects. Neurol Res 1999;21:665–669.
16. Kuo TB, Chern CM, Sheng WY, et al. Frequency domain analysis of cerebral blood flow velocity and its correlation with arterial blood pressure. J Cereb Blood Flow Metab 1998;18:311–318.
17. Schroth G, Klose U. Cerebrospinal fluid flow. II. Physiology of respiration-related pulsations. Neuroradiology 1992;35:10–15.
18. Aaslid R, Newell DW, Stooss R, et al. Assessment of cerebral autoregulation dynamics from simultaneous arterial and venous transcranial Doppler recordings in humans [Comments]. Stroke 1991; 22:1148–1154.
19. Kjällquist A, Lundberg N, Ponten U. Respiratory and cardiovascular changes during rapid spontaneous variations of ventricular fluid pressure in patients with intracranial hypertension. Acta Neurol Scand 1961;40:291–317.